Journal of Medicinal Chemistry

Article

pubs.acs.org/jmc

Virtual Screening and Computational Optimization for the Discovery of Covalent Prolyl Oligopeptidase Inhibitors with Activity in Human Cells

Stéphane De Cesco,[†] Sébastien Deslandes,[†] Eric Therrien,[†] David Levan,[†] Mickaël Cueto,[†] Ralf Schmidt,[‡] Louis-David Cantin,[‡] Anthony Mittermaier,[†] Lucienne Juillerat-Jeanneret,[§] and Nicolas Moitessier*[,†]

[†]Department of Chemistry, McGill University, 801 Sherbrooke Street West, Montréal, Québec H3A 0B8, Canada

[‡]AstraZeneca R&D Montréal, 7171 Frédérick-Banting, St. Laurent, Québec H4S 1Z9, Canada

[§]University Institute of Pathology, CHUV-UNIL, Rue du Bugnon 25, CH-1011, Lausanne, Switzerland

Supporting Information

ABSTRACT: Our docking program, Fitted, implemented in our computational platform, Forecaster, has been modified to carry out automated virtual screening of covalent inhibitors. With this modified version of the program, virtual screening and further docking-based optimization of a selected hit led to the identification of potential covalent reversible inhibitors of prolyl oligopeptidase activity. After visual inspection, a virtual hit molecule together with four analogues were selected for synthesis and made in one−five chemical steps. Biological evaluations on recombinant POP and FAPα enzymes, cell extracts, and living cells demonstrated high potency and selectivity for POP over FAPα and DPPIV. Three compounds even exhibited high nanomolar inhibitory activities in intact living human cells and acceptable metabolic stability. This small set of molecules also demonstrated that covalent binding and/or geometrical constraints to the ligand/protein complex may lead to an increase in bioactivity.

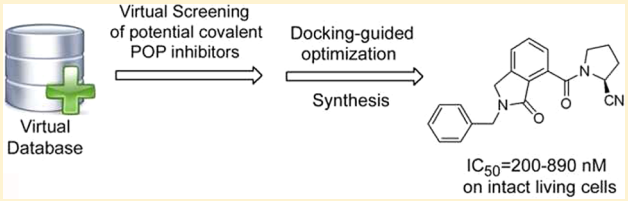

INTRODUCTION

Prolyl oligopeptidase (POP/PREP) is a highly conserved and widely distributed postproline endopeptidase. This enzyme, which can accommodate proline and alanine residues in its catalytic site, has been found to cleave neuropeptides in vitro.[1,2] POP was identified as a drug target soon after its discovery. For example, microorganism-derived POPs have been associated with the infectious potential of pathogens.[3] More importantly, it has been reported that POP is involved in many functions of the central nervous system and that abnormal POP activity, especially in the brain,[4] was associated with a number of diseases.[5−7] POP had first been implicated in memory impairment. More recently, the potential of POP inhibition in the treatment of neurodegenerative (e.g., Alzheimer's disease, Parkinson's disease) and psychiatric disorders (e.g., bipolar disorder[8]) has been revealed.[5,6,9] Although the function of POP remains unclear, POP inhibitors were tested in animal models and the role of POP in β-amyloid formation[10] and brain damage[11] was demonstrated.

As a result, POP inhibitors, either reversible covalent (e.g., Cbz-Gly-Prolinal, Cbz-Pro-Prolinal,[12] JTP-4819[13,14]) or non-covalent (e.g., SUAM-1221[15] and S-17092[16]), have already been prepared and evaluated in various experimental models with promising results (Figure 1).[9,17] Indeed, researchers have been able to measure beneficial effects, and recovery in some cases, on memory and learning abilities in animal models of brain disorders, along with prevention of amyloid-like depositions.[10,14,18,19] The latter observation offers promise of the relevance of this mechanism in Alzheimer's disease. However, despite these encouraging results, POP inhibitors have yet to enter advanced clinical trials (e.g., proof-of-concept

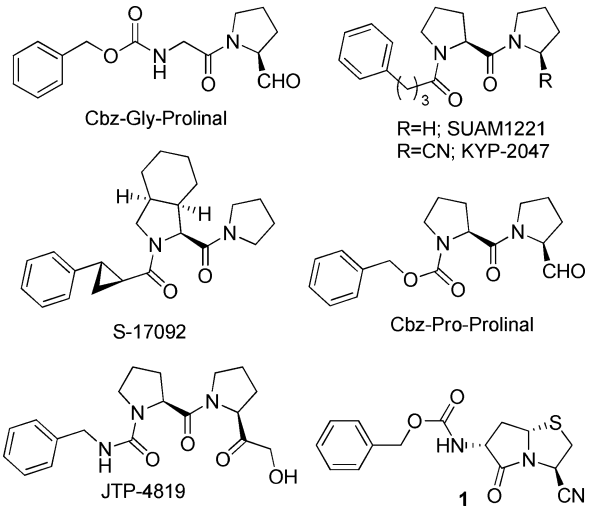

Figure 1. Selected known POP inhibitors.

Received: February 20, 2012

   dx.doi.org/10.1021/jm3002839 | J. Med. Chem. XXXX, XXX, XXX−XXX

studies). As discussed in a perspective article, the lack of data on the penetration of these reported inhibitors into the brain is a significant limitation for further development of clinically active POP inhibitors.[9] In fact, the first report on brain penetration was only disclosed last year by Jalkanen and co-workers, who demonstrated that JTP-4819, a compound which had been evaluated in phase I clinical trials,[20] was poorly distributed in the brain. A close analogue, KYP-2047 (Figure 1), exhibited more effective inhibition of intracellular POP.[21]

We became interested in developing novel scaffolds targeting POP that would have physiochemical properties suitable for further investigation and development. Our initial contributions to this field led to the design and synthesis of a first-generation constrained prolyl oligopeptidase inhibitor (**1**, Figure 1) exhibiting high nanomolar inhibitory potency in cell extract and low micromolar activity in intact living cells.[22] This first series was designed by structural modification of a known inhibitor. This ligand-based design was guided by docking of the proposed structures using our docking program, Fitted. Herein, we report the discovery of novel POP inhibitors using a very different strategy combining virtual screening and in silico optimization. We then describe their synthesis, biological evaluations, and metabolic stability.

Virtual Screening and Design. *Docking Covalent POP Inhibitors.* Literature reports support the formation of a covalent bond between the catalytic serine of the active site and a reactive functional group such as an aldehyde, hydroxyacetyl, or nitrile, present on the inhibitor.[23] The initial hypothesis, originally based on kinetic studies, was confirmed by X-ray crystallography of POP in complex with Cbz-Pro-Prolinal (PDB code: 1QFS[24]).

To fulfill this structural requirement, a fully automated virtual screening would therefore require the use of a program that is able to dock and model the formation of the covalent bond in the active site of the enzyme. Over the past decade, significant advances have brought the docking methods to the front line of drug design and discovery.[25] In fact, the number of reported docking methods and their successful applications to novel protein−ligand identification is ever-increasing. However, although some covalent drugs are reaching the market,[26] little effort has been devoted to the docking of such ligands. For instance, existing docking programs including GOLD,[27] AutoDock,[28] and FlexX[29] were modified to handle covalent inhibitors. However, all these programs require the manual definition of the ligand reacting functional groups, precluding their use in the context of virtual screening. To address this issue, our docking program, Fitted,[30,31] has been modified to automatically identify reactive functional groups appropriate for covalent inhibition and form covalent bonds when the catalytic serine and reactive groups are properly positioned. In 2009, we first described the use of Fitted for the design of covalent POP inhibitors.[22] To the best of our knowledge, MacDOCK[32] and Fitted are the only two programs considering covalent binding in a fully automated fashion. ICM was also modified to carry out a virtual screen of a large database of ketones and aldehydes on a cysteine protease but did not truly form a covalent bond. Rather, the catalytic cysteine side chain was removed and the protocol docked the stereomeric tetrahedral products which were built prior to the actual docking. To model the covalent binding, the protocol forced the tetrahedral adduct at the original position of the cysteine residue.[33] Interestingly, this procedure was very successful in identifying several ubiquitin-like poxvirus proteinase I7L inhibitors in a virtual screen.

Docking Covalent Inhibitors with Fitted. In its current version, Fitted first identifies the presence of aldehydes, ketones, boronates, and nitriles as functional groups while the protein residue capable of covalent binding is specified ahead of time (in the form of a keyword). The program then selects either the covalent or noncovalent mode by measuring the distance between the reactive carbon or boron and the catalytic residue. If this distance is below a threshold dependent on the reactive group (e.g., the covalent ideal bond distance as defined in the GAFF force field[34] plus 1 Å), the covalent bond is made, and additional bonds are either cleaved (O−H in Serine) or formed (O−H in hemiacetal, His-H if the inhibitor is a boronate) (Figure 2). All these steps are fully automated and

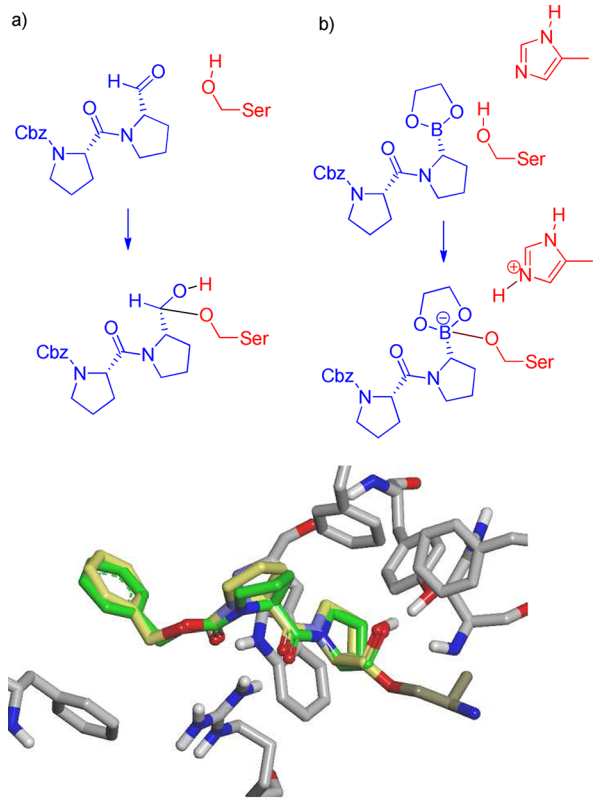

Figure 2. Chemical processes modeled in Fitted. (a) Formation of hemiacetal from aldehyde. (b) Formation of borate from boronate ester. (c) Application to the docking of Cbz-Pro-prolinal: yellow, docked; green, experimentally determined (X-ray crystal structure, PDB code: 1QFS).

do not require additional user intervention. As soon as a binding mode is proposed, it is scored. The current version of the RankScore scoring function[35] implemented in Fitted has not been modified to account for covalent bond formation and reactivity of the inhibitor, a major limitation of state-of-the-art docking program. In practice, our current scoring function will only evaluate the fit between the investigated inhibitors and POP. We expect its accuracy to be sufficient to discriminate active from inactive compounds. However, ranking based on predicted relative potency for active compounds would not be possible. Virtual screening with known inhibitors will validate this assumption (see below). Initial validation of Fitted with POP inhibitors and other covalent inhibitors demonstrated its accuracy in generating accurate binding modes as illustrated in

dx.doi.org/10.1021/jm3002839 | J. Med. Chem. XXXX, XXX, XXX−XXX

Figure 2c. Protein flexibility as implemented in Fitted can also be used in conjunction with the docking of covalent inhibitors.

Application to Virtual Screening. This version of our docking program was next implemented in our platform Forecaster[36] and used to screen potential POP inhibitors. The objective of this study was twofold. First, we aimed to discover novel POP inhibitors through virtual screening, then we also validated the covalent docking implementation in Fitted and its ability to discriminate active from inactive inhibitors. The designed workflow of actions is shown in Figure 3. First, a library of drug-like molecules was collected from the ZINC database[37,38] upon a substructure search for compounds containing either an aldehyde or a nitrile group. Descriptors such as the presence of a set of functional groups or molecular weight were next added to all the molecules and were used to filter out undesired molecules. These descriptors available in Forecaster are described in detail in a recent report and will not be discussed further herein.[36] For this purpose, our program, Reduce, was used to "Filter" (i.e., discard) any molecules featuring undesired functional groups (e.g., more than one potential covalent group or isocyanate) or violating the Lipinski's rules.[36] This process yielded a total of 2798 molecules. To evaluate the ability to identify POP inhibitors, nine known inhibitors (given as Supporting Information) were included in this library by merging the files from the filtered library with a separate file containing these nine known POP inhibitors. This extended library was then prepared for docking and screened using the Fitted program. On the right branch of the workflow shown in Figure 3, a crystal structure of POP bound to an inhibitor was used (PDB code: 2XDW). It was first converted from the PDB format into a format useable by our platform (e.g., Forecaster adds hydrogen atoms, atomic partial charges, atom types, checks for errors, orients water molecules and polar residue side chains) and then prepared for docking. The compounds were next docked into POP by Fitted in the rigid protein mode. Although this may look like a complex procedure, all these steps are simply selecting potential inhibitors on one side and preparing the protein on the other side and then using these structures for docking, all these steps being fully automated in the platform.[36] The docked compounds were finally rank-ordered by scores, revealing that the nine known inhibitors were ranked on the very top of the list (within the top 1.5%, see Supporting Information), indicating that Fitted was indeed able to discriminate active covalent POP inhibitors from potentially inactive molecules.

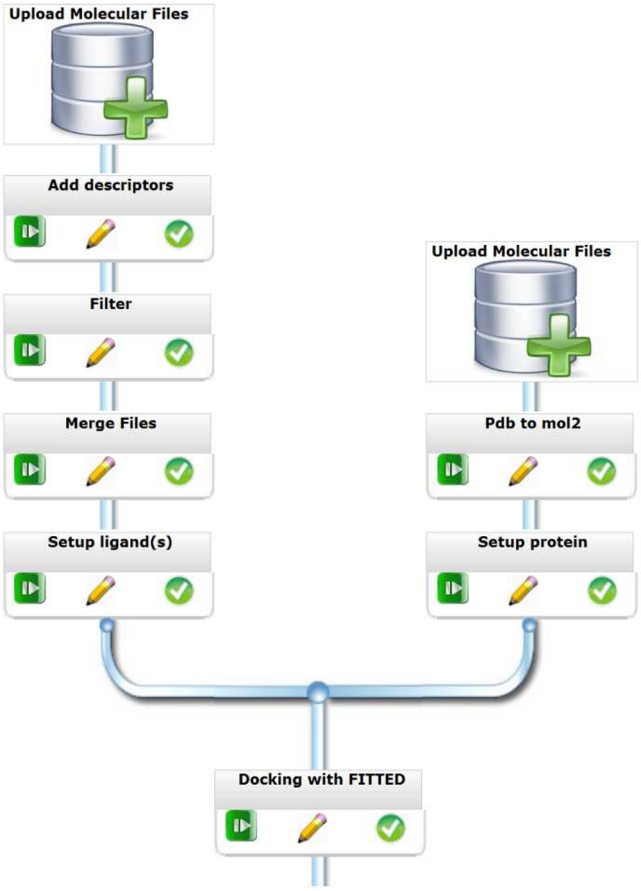

Figure 3. Workflow of actions used to identify potential covalent POP inhibitors.

The rank-ordered screened library was next analyzed in the hope to extract information that could be transposed into an active molecule. Analysis of the high scoring compounds allowed the identification of compound **2** as illustrated in the top panel of Figure 4. Visual inspection of the docked pose of **2** guided further structural modifications in order to make improved interactions with the enzyme. Optimization of **2** was conducted with respect to the pharmacophore we previously proposed which includes the need for two hydrogen bonds with Trp595 and Arg643 for optimal binding.[7] Docking followed by visual inspection of the poses validated the structural modifications. Key modifications were (1) the inversion of the amide bond, (2) rigidification of the ethyl group of **2** by introduction of a pyrrolidine ring, (3) rigidification of the scaffold by forming a five-membered ring on the left side, and (4) introduction of a nitrile in place of the aldehyde of compound **2** for covalent bond formation.

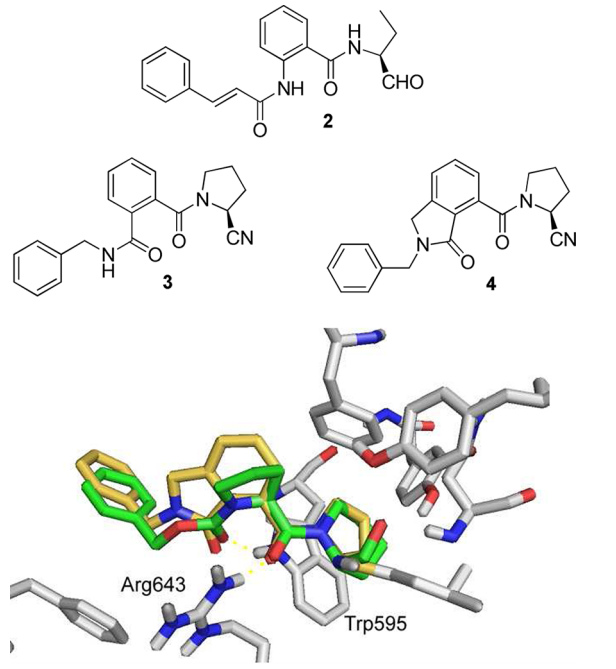

Figure 4. Top panel: potential hit discovered by virtual screening (**2**), designed potential inhibitors **3** and **4**. Bottom panel: compound **4** docked (yellow sticks) superposed with cocrystallized synthetic unnatural dipeptide (green sticks) and POP. (PDB code: 2XDW).

dx.doi.org/10.1021/jm3002839 | J. Med. Chem. XXXX, XXX, XXX−XXX

Compound **3** is the result of modifications **1**, **2**, and **4**, while compound **4** is the result of all of the four modifications. The bottom panel of Figure 4 shows the docking pose obtained for compound **4** superposed on a cocrystallized ligand with POP (PDB code: 2XDW).

Synthesis. To evaluate the impact of the rigidification (**3** into **4**) on the biological activity and confirm the presence of a covalent bond, **3**, **4**, and three analogues were selected for synthesis. The synthesis of the acyclic analogue **3** is depicted in Scheme 1. Phthalic anhydride **5** was first reacted with

Scheme 1[a]

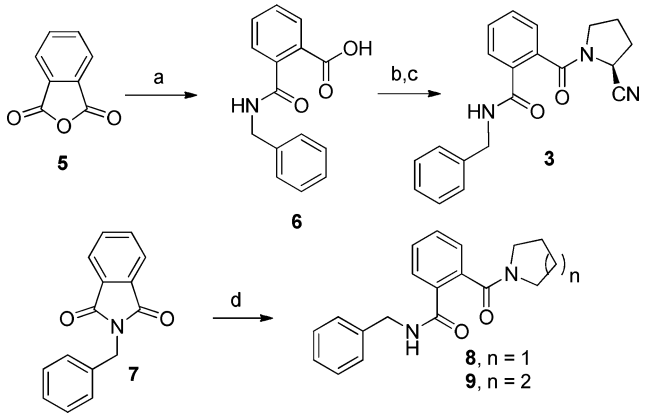

[a](a) Benzylamine, acetone, 60%; (b) BOP, Et_3N, H-Pro-NH_2, MeCN, 70%; (c) TFAA, Et_3N, THF, 77%; (d) pyrrolidine, 85%; or piperidine, 55%.

benzylamine to yield the corresponding benzoic acid **6** in reasonable yield. The carboxylic acid **6** was next coupled with L-prolinamide in presence of benzotriazole-1-yl-oxy-tris-(dimethylamino)-phosphonium hexafluorophosphate (BOP) and further converted to the nitrile derivative **3** upon dehydration of the terminal amide with trifluoroacetic anhydride. Although coupling 2-(*S*)-cyano-pyrrolidine with **6** would have saved a chemical step, it was found to be low yielding. In parallel, the potential noncovalent inhibitor **8**, an analogue of **3**, was obtained in a single step by condensation of commercially available *N*-benzylphthalimide and pyrrolidine. This compound stems from two of the above-mentioned modifications (inversion of the amide bond of compound **2** and rigidification of its ethyl group by introduction of a pyrrolidine ring). The six-membered ring analogue **9** was also synthesized in a similar manner using piperidine as a nucleophile.

The synthesis of the bicyclic series started with a reductive amination between furfural **10** and benzylamine producing the amine **11** (Scheme 2). This was followed by a tandem condensation with maleic anhydride/Diels–Alder cycloaddition to afford the carboxylic acid **12**. This intermediate underwent dehydration/rearomatization reaction to yield **13** upon acidic treatment. The synthesis was completed by conversion of the carboxylic acid **13** into the potential POP inhibitor **14** by coupling with pyrrolidine. Following a similar approach, the designed bicyclic inhibitor **4** was obtained through the coupling of **13** with 2-(*S*)-cyano-pyrrolidine.

RESULTS AND DISCUSSION

Inhibitory Potency. The inhibitory potency of these five compounds was assessed first in cell extracts of human glioblastoma cells and brain-derived endothelial cells, then in

Scheme 2[a]

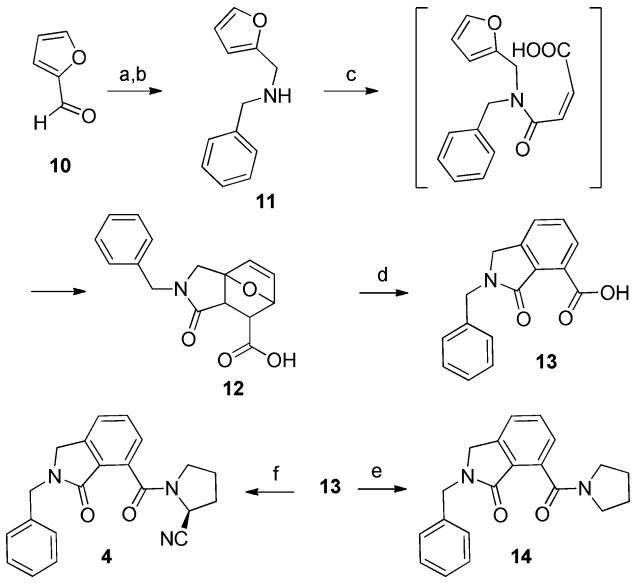

[a](a) Benzylamine, toluene, reflux; (b) $NaBH_3CN$, TFA, MeOH, 45% (over 2 steps); (c) maleic anhydride, toluene, reflux, 86%; (d) HCl conc reflux, 78%; (e) Piv-Cl, Et_3N, pyrrolidine, 63%; (f) BOP, Et_3N, DMF, 2-(*S*)-cyano-pyrrolidine, TFA, 72%.

intact living cells (Tables 1–2), expressing POP and DPPIV activities. A fluorigenic POP specific substrate (Cbz-Gly-Pro-AMC) was used to measure the POP activity while DPPIV activity was measured using Gly-Pro-AMC.[22] DPPIV is a prolyl-aminodipeptidase which cleaves dipeptides with free *N*-terminus and a proline residue at position 2 on the *N*-terminus side. This activity, which is targeted for the treatment of diabetes type II, should not be modulated by POP inhibitors.[9] As shown in Table 1, four of the five tested compounds

Table 1. Inhibition of POP and DPPIV Activity in Cell Extracts[a]

compd	LN18, LN229, LNZ308[b]	HCEC[c]
3	+++	+++
8	+++	+++
9	++	++
4	+++	+++
14	+++	+++

[a]++, >50% inhibition at 100 μM; +++, >90% inhibition at 20 μM. [b]LN18, LN229, LNZ308: human glioblastoma cells. [c]HCEC, human brain-derived endothelial cells.

exhibited significant POP inhibitory potency at a concentration of 20 μM in cell extracts. In addition, none inhibited the DPPIV activity at concentration as high as 100 μM. In addition, the measured potency is consistent throughout the cell lines. We have previously found that substituting the five-membered ring with a six-membered ring was detrimental to the inhibitor's activity (Figure 5).[22] This contrasted with the finding from Racys and co-workers who reported a very active inhibitor built around a piperidine ring.[39] In the present work, the substitution of the pyrrolidine ring of **8** by a piperidine ring (**9**) led to a decrease of inhibitory activity.

With these promising results in hand, these five active compounds were further assessed for their inhibitory activity in intact living cells (Tables 2 and 3 and Figure 6). This second

dx.doi.org/10.1021/jm3002839 | J. Med. Chem. XXXX, XXX, XXX–XXX

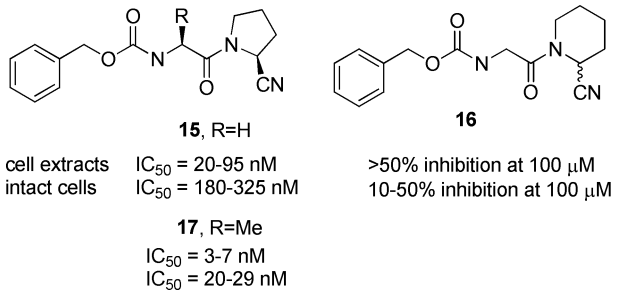

Figure 5. Ring Size and Inhibitory Potency against POP.[22]

Table 2. Inhibition of POP Activity in Living Intact Cells.[a]

compd	LN18, LN229, LNZ308[b]	HCEC[c]
3	+++	+++
8	++	++
9	–	–
4	+++	+++
14	+++	+++

[a] –, No inhibition at 100 μM; ++, >50% inhibition at 100 μM; +++, >90% inhibition at 20 μM. [b] LN18, LN229, LNZ308: human glioblastoma cells. [c] HCEC, human brain-derived endothelial cells.

set of experiments assessed the intracellular inhibition of POP activity by these small molecules. The inhibition of DPPIV-like activity by the compounds was not determined in intact cells because no inhibition had been found in cell extracts. These experiments demonstrated that not only are these compounds inhibiting the POP activity, but they are also able to penetrate the cells. To further evaluate their inhibitory potency, dose response efficacy of the three more potent inhibitors, compounds **3**, **4**, and **14**, were compared (Figure 6) and IC_{50} values determined (Table 3) in intact cells and in cell extracts We were also very pleased to see that three of these compounds remain in the nanomolar range while going from cell extracts to living cells while our previous series illustrated by compound **1** were active in the low micromolar range under the same conditions. However, we have previously identified Cbz-protected pseudopeptides (e.g., **17**, Figure 5) that exhibit better potency, showing that there is still room for improvement.

Comparing IC_{50} values between cell extracts and intact cells (Table 3) demonstrated an increased efficacy for the extracted enzyme for compounds **3** and **4**, but not **14**, compared to intact cells. This information suggests that cellular uptake may be a limiting factor for compounds **3** and **4**, but not **14**.

Selectivity. In addition to POP, the only enzyme with comparable prolyl-specific endoproteolytic enzymatic properties is FAPα.[40] The cells used, either human glioblastoma cells or human brain-derived endothelial cells, do not express FAPα (data not shown, Juillerat et al, manuscript in preparation), thus for these cells, either intact cells or cell extracts, selectivity is not an issue. To evaluate the selectivity of the inhibitors, inhibition of purified recombinant human POP/PREP and FAPα has been assessed and K_M determinations have been performed (Tables 4 and 5).

The experiments with purified recombinant human POP showed that the three selected inhibitors, compounds **3**, **4**, and **14**, are significantly better inhibitors of rhPOP than of rhFAPα (Table 4). This also demonstrated that K_M values for the rhPOP and for the enzyme activity in cell extracts (Table 5) are very similar. rhFAPα also displayed a much less favorable K_M for the selected substrate than rhPOP or the cell extracts. Thus, compounds **3**, **4**, and **14** proved to be very poor inhibitors for FAPα activity compared to POP. Therefore, we can conclude that the target enzyme in human brain-derived cells is POP/PREP and that the inhibitors **3**, **4**, and **14** are selective for POP versus FAPα.

Structure–Activity Relationship. The 2 orders of magnitude difference in activity between compounds **3** (IC_{50} = 65 nM, HCEC) and **8** (IC_{50} = 20–100 μM) in cell extracts might indicate the formation of a covalent bond as intended.

Overall, as shown in Figure 7, the geometrical constraint brought by the lactam ring (**8** into **14**) or the putative covalent bond made with the nitrile (**8** into **3**) were highly beneficial to the inhibitory activity against POP activity. Combining the two

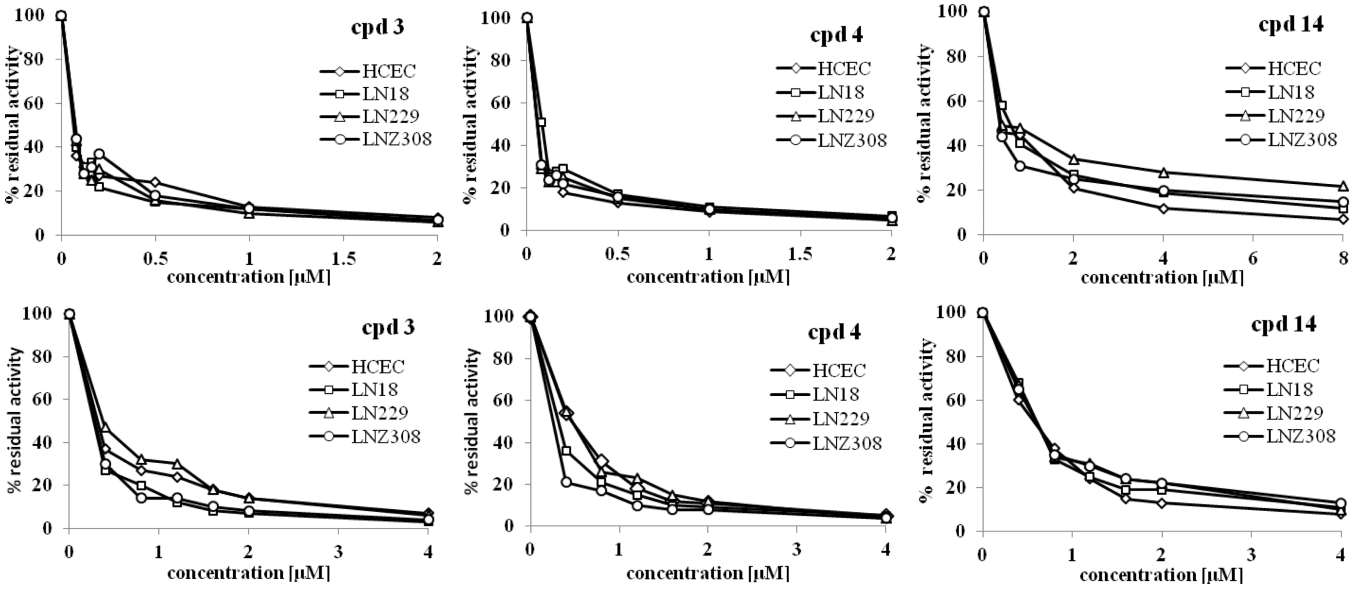

Figure 6. Dose–response inhibition of POP activity in cell extracts (top) and intact human endothelial (HCEC) and glioblastoma (LN18, LN229, LNZ308) cells (bottom) by compounds **3**, **4**, and **14**.

dx.doi.org/10.1021/jm3002839 | J. Med. Chem. XXXX, XXX, XXX–XXX

Table 3. Inhibition of POP Activity (IC_{50}, [nM]) in Cell Extracts and Living Intact Cells

	cell extracts				intact living cells			
compd	LN18[a]	LN229[a]	LNZ308[a]	HCEC[b]	LN18[a]	LN229[a]	LNZ308[a]	HCEC[b]
1[22]	nd	500	200	700	nd	2000	2500	2000
3	68	68	73	65	250	500	290	290
4	81	45	45	45	300	450	200	500
14	620	500	350	620	580	610	640	680

[a]LN18, LN229, LNZ308: human glioblastoma cells. [b]HCEC, human brain-derived endothelial cells.

Table 4. Inhibition of Recombinant Human FAP-α and POP/PREP by Compounds 3, 4, and 14

	rhFAP-α		rhPOP/PREP	
compd	% @ 100 μM	IC_{50} (μM)	% @ 2 μM	IC_{50} (nM)
3	34	>100	90	<50
4	28	>100	93	<50
14	11	>100	63	= 150

structural changes (**14** into **4** or **3** into **4**) revealed that the additional lactam ring was not necessary for optimal binding as **4** is only slightly, but not significantly, more potent than **3**. When noncovalent binding occurs, introduction of a geometrical constraint in the form of a ring (**8** into **14**) reduces the entropy penalty of binding but often requires slight adjustments of the binding mode and/or of the protein environment to keep the same favorable interactions. However, when covalent binding occurs, a second constraint in the form of a covalent bond is added, precluding any adjustment of the binding mode through translation or rotation of the inhibitor. It may also affect protein flexibility which could result in an entropic penalty.[41] As a result, rigidification of **3** into **4** resulted in no significant gain in inhibitory activity. One can question whether the postulated covalent bond between the nitrile group and the protein catalytic serine actually occurs. Although additional work is needed to confirm this hypothesis, the large binding affinity increase observed when the nitrile is added onto **8** (IC_{50} = ca. 10000 nM) to form **3** (IC_{50} ca. 100 nM) strongly suggests the formation of a covalent bond as intended. Recently, crystal structures of nitrile-containing inhibitors including **18** have shown that indeed a covalent bond is formed with the catalytic serine of POP (Figure 8).[42] As with our compound **4**, this compound **18** features a cyanopyrrolidine ring.

Metabolic Stability. Prior to testing these compounds in vivo, we thought to assess their metabolic stability in human liver microsomes (HLM) (Table 6 and Figure 9). As the following step would be to test these inhibitors in animals, metabolism was also evaluated on rat liver microsomes (RLM). The derivatives **8** and **9** were first assessed and revealed major oxidation of the pyrrolidine ring on the right-hand side of these inhibitors and minor *N*-debenzylation or aromatic oxidation on the left-hand side of the compounds.

A close look at the metabolic stability revealed that compared to the first generation constrained prolyl oligopeptidase inhibitor **1**, constrained compounds **4** and **14** maintained similar metabolic stability whereas the corresponding less restricted analogues **3**, **8**, and **9** exhibited increased metabolic liabilities. We believe that the geometrical constrains of compounds **1**, **4**, and **14** affects the recognition by metabolic enzymes (i.e., cytochrome P450 enzymes), while the more flexible compounds **3**, **8**, and **9** may adopt more favorable conformations for recognition by cytochrome P450 enzymes.

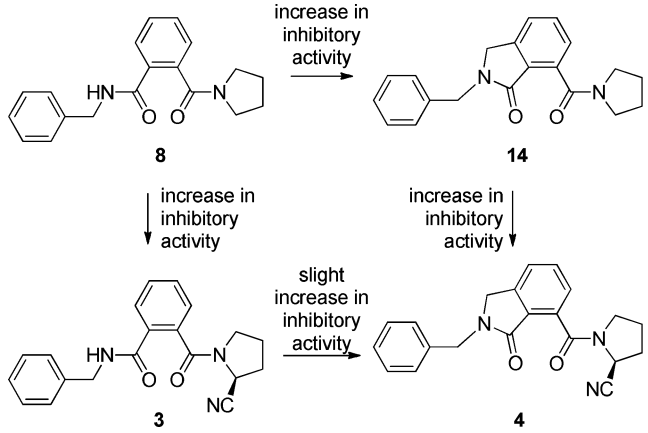

Figure 7. Structure–activity relationships in cell extracts.

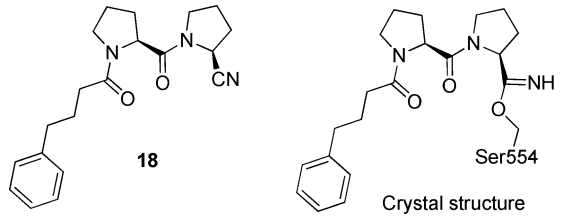

Figure 8. Cocrystallized covalent POP inhibitor.

Table 6. In Vitro Metabolic Stability in Human and Rat Liver Microsomes

	HLM		RLM	
compd	in vitro Clint (μL/min/mg)	in vitro $t_{1/2}$ (min)	in vitro Clint (μL/min/mg))	in vitro $t_{1/2}$ (min)
1	10	134	nt[a]	nt[a]
3	44	31	37	38
4	13	111	39	35
8	25	55	83	17
9	89	16	311	4
14	14	98	62	23

[a]Not tested.

Table 5. K_M [mM] Values of Recombinant Human POP/PREP and FAPα for the Substrate

compd	LN18	LN229	LNZ308	HCEC	rhPOP/PREP	rhFAP-α
Z-Gly-Pro-AMC	0.0085	0.0067	0.0081	0.0070	0.0085	0.103

dx.doi.org/10.1021/jm3002839 | J. Med. Chem. XXXX, XXX, XXX–XXX

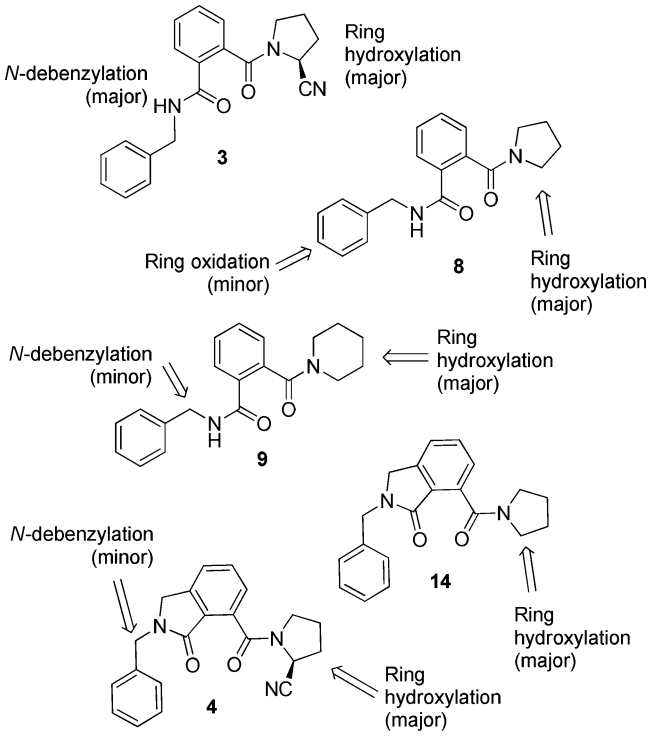

Figure 9. Metabolic stability in human and rat liver microsomes.

To pinpoint the site of metabolism, metabolite identification experiments were performed for all analogues (Figure 8). The analysis revealed that, with exception of compound **3**, multiple oxidations of the pyrrolidine ring are mainly responsible for the metabolic clearance, even more pronounced for analogue **9** containing a piperidine moiety. The main metabolite pathway for analogue **3** led to a debenzylated metabolite.

CONCLUSION

The discovery of novel inhibitors of POP activity selective over DPPIV activity was made possible through the combination of virtual screening (hit identification) using Fitted, a docking program considering covalent bond formation, virtual lead optimization, synthesis, and biological evaluation. The medicinal chemist/docking-guided lead optimization ensures that both predicted binding affinity and synthetic feasibility were optimal. Thus a selection of five molecules was synthesized in one (**8** and **9**), three (**3**), or five (**4** and **13**) chemical steps. This study represents one of the rare virtual screening studies applied to the discovery of covalent inhibitors. Interestingly, with focused synthetic efforts, we were able to develop three inhibitors that are 10 times more active intracellularly than was our previous hit molecule **1**, which required significantly more synthesis efforts.[22] Further investigation using recombinant POP enzyme confirmed that POP is the target of these inhibitors and that they are highly selective for POP over FAPα. While the introduction of one geometrical constraint (either a lactam ring or a reactive group) was found to increase the inhibitory potency, the combination of the two modifications did not produce the expected synergistic increase. In addition, metabolism studies revealed an acceptable microsomal stability for the bicyclic analogues at this stage, a promising indication for further in vivo evaluation.

EXPERIMENTAL SECTION

Virtual Screening. The database of small molecules was downloaded from the ZINC Web site (http://zinc.docking.org) and further processed using a series of programs implemented in our platform Forecaster.[36] First, the library was subjected to filtering using Reduce (formal charge: [−1,0], molecular weight [200,550], aldehyde [0,1], should not include the following functional group: ester, primary amine, acyl chloride, ketone, hydroxamate, isocyanide, azide). The resulting compounds were next prepared for docking and docked to a protein structure prepared from the PDB file using Prepare (PDB code: 2XDW) and prepared for docking using Process. The docking was carried out with Ser554 identified as a catalytic residue susceptible to forming a covalent bond with reactive groups.

Synthesis. All commercially available reagents were used without further purification unless otherwise stated. FTIR spectra were recorded using a Perkin-Elmer Spectrum One FT-IR. ^{1}H and ^{13}C NMR spectra were recorded on Varian Mercury 400 MHz, 300 MHz, or Unity 500 spectrometers. Chemical shifts are reported in ppm using the residual of deuterated solvents as an internal standard. Thin layer chromatography visualization was performed by UV or by development using $KMnO_4$, H_2SO_4/MeOH, or cerium/molybdate solutions. Chromatography was performed on silica gel 60 (230−40 mesh). Low resolution mass spectrometry was performed by ESI using a Thermoquest Finnigan LCQ Duo. High resolution mass spectrometry was performed by EI peak matching (70 eV) on a Kratos MS25 RFA double focusing mass spectrometer or by ESI on a Ion Spec 7.0 T FTMS at McGill University. Prior to biological testing, reversed phase HPLC was used to verify the purity of compounds on an Agilent 1100 series instrument equipped with VWD-detector, C18 reverse column (Agilent, Zorbax Eclipse XDB-C18 150 mm × 4.6 mm, 5 μm), UV detection at 254 nm. All tested compounds were at least 95% pure.

(*S*)-*N*-Benzyl-2-(2-cyanopyrrolidine-1-carbonyl)benzamide (3). To a stirred solution of the carboxylic acid compound **6**[43] (500 mg, 1.96 mmol), in MeCN (50 mL) under argon atmosphere, were added sequentially BOP (1.04 g, 2.3 mmol), L-prolinamide (0.224 g, 1.96 mmol), and Et_3N (601 μL, 4.4 mmol). The reaction mixture was allowed to react for 15 h at room temperature. The reaction mixture was quenched with a 10% HCl solution, extracted in EtOAc, and washed successively with saturated $NaHCO_3$, and brine. The organic phase was dried over anhydrous Na_2SO_4, filtered, and concentrated in vacuo to afford (*S*)-1-(2-(benzylcarbamoyl)benzoyl)pyrrolidine-2-carboxamide. Without further purification. the amide was dissolved in DCM (60 mL) and Et_3N (863 μL, 6.2 mmol) was added. The resulting solution was cooled down to 0 °C, and then TFAA (564 μL, 4 mmol) was added dropwise. After stirring for another 2 h, a saturated solution of $NaHCO_3$ was added and the organic phase was dried over Na_2SO_4, and concentrated in vacuo to afford, after flash chromatography (EtOAc/hexanes, 1:1), compound **3** (250 mg, 55%, white solid); R_f = 0.10 (EtOAc/hexanes, 1:1). IR (film) υ max 3311, 2925, 1633, 1404, 1303, 698 cm^{-1}; $[\alpha]_D^{20}$ = −5.4 (*c* 1.25, $CHCl_3$). ^{1}H NMR (400 MHz, $CDCl_3$, 3:1 mixture of rotamers) δ 1.91−2.30 (m, 4H), 3.19−3.33 (m, 1.3H), 3.55−3.69 (m, 0.7H), 4.42 (m, 1H), 4.55 (d, 0.75H, *J* = 6.6 Hz), 4.69 (m, 1H), 4.73 (d, 0.25H, *J* = 6.6 Hz), 6.69 (bs, 0.25H), 6.85 (bs, 0.75H), 7.27−7.74 (m, 9H). ^{13}C NMR (75 MHz, MeOD) δ 172.59, 169.57, 140.07, 137.72, 134.53, 132.53, 130.98, 129.73 (2C), 128.85 (2C), 128.77, 128.40, 128.23, 119.75, 49.96, 47.65, 44.67, 31.65, 26.07. HRMS (ESI+) calcd for $[C_{20}H_{19}N_3O_2 + H]^+$, 334.15500; found, 334.15454;

***N*-Benzyl-2-(pyrrolidine-1-carbonyl)benzamide (8).** To a solution of benzylphthalimide (503 mg, 2.13 mmol) in THF (15 mL) was added pyrrolidine (0.20 mL, 2.41 mmol). The reaction vessel was left to react for 24 h under argon atmosphere. The mixture was evaporated to dryness in vacuo, and the final product was obtained after recrystallization from methanol (551 mg, 85%). The ^{1}H NMR (400 MHz, DMSO-d_6) was identical to the previously reported data.[44] ^{1}H NMR (400 MHz, DMSO-d_6): δ 1.70−1.83 (m, 4 H), 3.06 (t, 2 H, *J* = 6.7 Hz), 3.36 (t, 2 H, *J* = 6.7 Hz), 4.41 (d, 2 H, *J* = 6.0 Hz), 7.23−7.33 (m, 6 H), 7.44−7.53 (m, 2 H), 7.65 (d, 1 H, *J* = 7.4 Hz), 8.89 (t,

dx.doi.org/10.1021/jm3002839 | J. Med. Chem. XXXX, XXX, XXX−XXX

1 H, J = 5.8 Hz). HRMS (ESI+) calcd for $[C_{19}H_{20}N_2O_2 + Na]^+$, 331.14170; found, 331.14244.

***N*-Benzyl-2-(piperidine-1-carbonyl)benzamide (9).** To a solution of benzylphthalimide (0.462 g, 1.95 mmol) in THF (20 mL) was added piperidine (0.20 mL, 2.02 mmol). The reaction vessel was set aside for 92 h under argon atmosphere. The mixture was evaporated to dryness in vacuo, and the final product (0.346 g, 55%) was obtained by flash column chromatography (1:1 hexanes/ethyl acetate, R_f = 0.13). ^{1}H NMR (400 MHz, DMSO-d_6) δ 1.20−1.43 (m, 6H), 2.95 (bs, 2H), 3.31−3.49 (m, 2H), 4.33 (d, 2H, J = 6.0 Hz), 7.14−7.18 (m, 2 H), 7.25 (s, 2H), 7.26 (s, 2H), 7.36−7.45 (m, 2H), 7.58 (dd, 1H, J = 7.6, 1.3 Hz), 8.81 (t, 1H, J = 6.0 Hz). ^{13}C NMR (75 MHz, $CDCl_3$) δ 169.83, 167.31, 138.28, 135.04, 132.82, 130.78, 129.38, 128.97, 128.60 (2C), 127.91 (2C), 127.35, 125.85, 48.45, 43.94, 42.62, 26.10, 25.37, 24.31. HRMS (ESI+) calcd for $[C_{20}H_{22}N_2O_2 + Na]^+$, 345.15735; found, 345.15823. IR (film) υ max 3305, 2938, 2856, 2350,1600, 1596, 1490 cm^{-1}.

***N*-Benzyl-1-(furan-2-yl)methanamine (11).** A mixture of furan-2-carboxaldehyde (1.3 mL, 15.6 mmol) and benzylamine (1.79 mL, 16.39 mmol) in benzene (31 mL) was heated at reflux with a Dean−Stark for 4 h. The solvent was evaporated to dryness, and the crude imine was dissolved in MeOH (15 mL) and then cooled to 0 °C. Sodium cyanoborohydride (1.47 g, 23.4 mmol) and trifluoroacetic acid (1.26 mL, 16.4 mmol) were added successively to the mixture. After 30 min, the mixture was allowed to warm to room temperature, and stirring was continued for a further 2 h. The mixture was evaporated under reduced pressure and the residue dissolved in EtOAc (20 mL) and washed with 1 M NaOH (10 mL) and saturated NaCl solution (10 mL). The organic phase was dried over Na_2SO_4 and concentrated in vacuo. The residue was purified by flash chromatography (EtOAc/hexanes, 1:4, R_f = 0.15) to afford **11** (1.32 g, 45%, light-yellow oil). IR (film) υ max 3063, 3028, 2831, 1602, 1496, 1454, 1360, 1335, 1146, 1008, 730, 697 cm^{-1}. ^{1}H NMR (300 MHz, $CDCl_3$) δ 1.73 (s, 1H), 3.80 (s, 4H), 6.20 (s, 1H), 6.33 (s, 1H), 7.23−7.38 (m, 6H). ^{13}C NMR (75 MHz, $CDCl_3$) δ 153.82, 141.83, 139.90, 128.42, 128.27, 127.03, 110.11, 107.05, 52.80, 45.37. HRMS (ESI+) calcd for $[C_{12}H_{13}NO + H]^+$, 188.10699; found, 188.10692.

2-Benzyl-1-oxo-1,2,3,6,7,7a-hexahydro-3a,6-epoxyisoindole-7-carboxylic Acid (12). To a stirred solution of **11** (1.30 g, 6.94 mmol) in toluene (100 mL), maleic anhydride (0.68 g, 6.94 mmol) was added, and the resulting mixture was heated to reflux for 5 h. The mixture was cooled to room temperature and further stirred overnight. The precipitate was collected by filtration, washed with Et_2O (25 mL), and dried under vacuum. The product **12** (1.71 g, 86%) was isolated as a white solid. IR (film) υ max 3030, 1734, 1658, 1477, 1359, 1206 cm^{-1}; mp ($CHCl_3$) 170−174 °C. ^{1}H NMR (300 MHz, $CDCl_3$) δ 2.84 (d, 1H, J = 9.0 Hz), 2.98 (d, 1H, J = 9.0 Hz), 3.65 (d, 1H, J = 12.0 Hz), 3.83 (d, 1H, J = 12.0 Hz), 4.42 (d, 1H, J = 15.0 Hz), 4.63 (d, 1H, J = 15.0 Hz), 5.24 (s, 1H), 6.41 (s, 2H), 7.28−7.32 (m, 5H), 10.77 (bs, 1H). ^{13}C NMR (75 MHz, $CDCl_3$) δ 173.58, 172.50, 137.08, 135.28, 134.99, 128.90, 127.93, 127.80, 88.68, 82.17, 51.01, 48.51, 46.97, 45.50. HRMS (ESI+) calcd for $[C_{16}H_{15}NO_4 + H]^+$, 286.10738; found, 286.10696.

2-Benzyl-3-oxoisoindoline-4-carboxylic Acid (13). A solution of compound **12** (1.70 g, 5.96 mmol) was dissolved in concd HCl (30 mL) and refluxed for 3 h. The mixture was then cooled to room temperature, stirred overnight, and concentrated in vacuo. MeOH (20 mL) was added, and the solid was collected by filtration affording compound **13** (1.25 g, 78%, tan solid). IR (film) υ max 3046, 1869, 1708, 1598, 1579, 1496 cm^{-1}; mp ($CHCl_3$) 178−182 °C. ^{1}H NMR (300 MHz, $CDCl_3$) δ 4.44 (s, 2H), 4.86 (s, 2H), 7.32−7.40 (m, 5H), 7.62 (d, 1H, J = 6.0 Hz), 7.68 (t, 1H, J = 6.0 Hz), 8.40 (d, 1H, J = 9.0 Hz). ^{13}C NMR (75 MHz, $CDCl_3$) δ 169.53, 165.41, 141.89, 135.07, 133.31, 132.35, 129.35, 129.22, 129.08, 128.37, 128.32, 126.99, 50.41, 47.24. HRMS (ESI+) calcd for $[C_{16}H_{14}NO_3 + Na]^+$, 268.09682; found, 268.09644.

2-Benzyl-7-(pyrrolidine-1-carbonyl)isoindolin-1-one (14). To a 0 °C solution of compound **5** (216 mg, 0.808 mmol) and Et_3N (0.12 mL, 0.889 mmol) in DCM (2.0 mL) was added dropwise a solution of pivaloyl chloride (0.10 mL, 0.808 mmol) in DCM (1.0 mL). The mixture was stirred at 0 °C for 1 h, followed by the addition of a solution of pyrrolidine (0.07 mL, 0.889 mmol) and Et_3N (0.12 mL, 0.889 mmol) in DCM (1.0 mL). After stirring for a further 2 h at 0 °C, the mixture was allowed to warm to room temperature and stirring was continued overnight. The reaction mixture was quenched with a 10% HCl solution (15 mL), extracted with DCM, dried over Na_2SO_4, and evaporated under reduced pressure to afford, after flash chromatography (EtOAc/hexanes 4:1 to 1:0, R_f = 0.10), compound **14** (163 mg, 63%, white solid). IR (film) υ max 2968, 2925, 2875,1685, 1629, 1437 cm^{-1}. ^{1}H NMR (300 MHz, $CDCl_3$) δ 1.91−1.96 (m, 4H), 3.06 (s, 1H), 3.24 (s, 1H), 3.65 (s, 1H), 3.80 (s, 1H), 4.21 (s, 2H), 4.61 (s, 1H), 4.84 (s, 1H), 7.23−7.36 (m, 7H), 7.50 (t, 1H, J = 6.0 Hz). ^{13}C NMR (75 MHz, $CDCl_3$) δ 167.05, 166.89, 141.79, 136.95, 136.00, 135.46, 131.82, 128.92 (2C) 128.40 (2C), 127.86, 126.20, 123.39, 49.34, 48.27, 46.46, 45.71, 26.02, 24.63. HRMS (ESI+) calcd for $[C_{20}H_{20}N_2O_2 + H]^+$, 321.15975; found. 321.15956.

(*S*)-1-(2-Benzyl-3-oxoisoindoline-4-carbonyl)pyrrolidine-2-carbonitrile (4). To a stirred solution of compound **5** (50 mg, 0.186 mmol) in DMF (1.0 mL) were added sequentially BOP (99 mg, 0.223 mmol), (*S*)-pyrrolidine-2-carbonitrile TFA salt (39 mg, 0.186 mmol), and Et_3N (0.06 mL, 0.408 mmol). The mixture was stirred for 15 h at room temperature and quenched with a 10% HCl solution (10 mL), extracted with EtOAc, dried over Na_2SO_4, and concentrated in vacuo to afford, after flash chromatography (EtOAc/hexanes, 7:3, R_f = 0.22), compound **4** (59 mg, 92%, white solid). ^{1}H NMR (500 MHz, acetone-d_6) δ 2.01−2.44 (m, 4H), 3.29 (bs, 1.5H), 3.73 (m, 0.5H), 4.42 (s, 2H), 4.78 (m, 2H), 4.96 (m, 1H), 7.28−7.45 (m, 6H), 7.62−7.70 (m, 2H). ^{13}C NMR (75 MHz, $CDCl_3$) δ 167.72, 166.80, 141.86, 136.56, 133.03, 132.00, 128.96 (2C), 128.30 (2C), 127.92, 126.32, 124.47, 124.27, 118.77, 49.48, 48.96, 48.09, 46.45, 32.17 (0.3C), 30.41 (0.7C), 25.12 (0.7C), 23.50 (0.3C). IR (film) υ max 3014, 1681, 1636, 1413 cm^{-1}. HRMS (ESI+) calcd for $[C_{21}H_{19}N_3O_2 + H]^+$, 346.15500; found, 346.15468.

Inhibitory Potency. The human glioblastoma-derived cell lines LN18, LN229, and LNZ308 were a kind gift of A. C. Diserens, Neurosurgery Department, Lausanne, Switzerland, the immortalized human brain-derived HCEC cells were kindly provided by D. Stanimirovic, Ottawa, Canada. Cells were grown in DMEM culture medium containing 4.5 g/L glucose, 10% fetal calf serum (FCS) (HCEC cells), or 5% FCS (LN18, LN229, and LNZ308 cells), and antibiotics (all from Gibco, Basel, Switzerland). One to two days before evaluation, cells were seeded in 48-well plates (Costar, Corning, NY) in complete medium in order to reach confluence on the day of experiment. On the day of experiment, the culture medium was removed, and either 200 μL of phosphate-buffered saline (PBS, pH 7.2−7.4) were added in half of the wells or 200 μL of PBS containing 0.1% Triton X-100 (Fluka, Buchs, Switzerland) were added in the other half of the wells for the evaluation of the inhibition of enzyme activities in intact cells or cell extracts, respectively. Experiments were performed in duplicate wells. The synthetic molecules were dissolved at 10 mg/mL in methanol and then diluted 1:10 in H_2O, and 1 or 5 μL of the water solution were added to duplicate PBS and PBS-Triton wells, followed after 5−10 min at room temperature by either 1 μL of Gly-Pro-AMC (DPPIV activity) or *Z*-Gly-Pro-AMC (POP activity) substrates (1 mg/mL DMSO, both from Bachem, Bubendorf, Switzerland), final concentration 10 μM. Increase in fluorescence at $\lambda_{ex}/\lambda_{em}$ = 360/460 nm was recorded for 30 min at 37 °C in a thermostatted multiwell fluorescence reader (Cytofluor, PerSeptive BioSystems, Switzerland). For the determination of IC_{50}, cells in PBS or in PBS-Triton X-100 were exposed to decreasing concentrations of the inhibitors, and then determination of residual activity was measured and plotted against inhibitor concentration. IC_{50} values were determined graphically.

Recombinant human prolyl oligopeptidase/PREP (rhPOP/PREP, 0.5 mg/mL, catalogue no. 4308-SE) and fibroblast activation protein α (rhFAPα, 0.5 mg/mL, catalogue no. 3715-SE) were obtained from R&D Systems (Abingdon, UK). The stock solutions were diluted in PBS containing 1 mg/mL bovine serum albumin (BSA, Sigma), a protein concentration comparable to the protein concentration of cell extracts. For comparison of inhibitory potencies, IC_{50} and K_M in cell

dx.doi.org/10.1021/jm3002839 | J. Med. Chem. XXXX, XXX, XXX−XXX

extracts with rhPOP/PREP and rhFAPα, cells were grown in 6 cm Petri dishes (Falcon, BD, Erembodegem, Belgium) and extracted in 3 mL of PBS-Triton (resulting in solutions of ~0.5 mg protein/mL). For the evaluation of the inhibition of the recombinant human enzymes, the experimental design was similar to the experimental design of cell extracts. For K_M determinations, increasing substrate concentrations were added to the cell extracts in PBS-Triton or to the recombinant enzymes in PBS-BSA, and the K_M values were determined graphically using a double-reciprocal Michaelis–Menten plot.

Metabolic Stability Assay (Clint). The test substances at 1 μM concentration were mixed with 0.1 M KH_2PO_4 buffer pH 7.4 and liver microsomes (BD-Gentest) at 0.5618 mg/mL in a 96-deep well plate and incubated at 37 °C. NADPH was added to start the reaction. After 0, 10, 20, and 30 min, an aliquot of the incubation mixture was transferred to a 384-well plate containing an equal amount of acetonitrile to stop the reaction. The 384-well plate was centrifuged for 30 min at 9000*g* and under cooling (4 °C). The supernatants were then analyzed on an Agilent 1100 LC-MSD system. The robot used for this assay is a TECAN Genesis (8-tip pipettes). All steps in the assay, i.e., pipetting, incubation, etc., were performed by the robot except for the centrifugation step.

Metabolite Identification. Sample preparation: Compounds were incubated at 50 μM with 1 mg/mL of human liver microsomes (BD-Gentest) in the presence of 1 mM NADPH at 37 °C for 30 min. After precipitation with acetonitrile and centrifugation, the supernatant diluted with water (1:1) was analyzed by LC/MS.

LC/MS conditions and data analysis: An Acquity UPLC/Q-TOF system (Waters) with UV detector was employed for data acquisition. Gradients made up from 10 mM ammonium formate buffer and MeCN at a flow of 0.5 mL/min were applied on a HSS T3 column (1.8 μm, 2.1 mm × 100 mm) connected to the mass spectrometer operating in positive electrospray ionization.

Q-TOF Premier MS^E method was used in full scan mode, and fragmentation data were obtained by collision energy ramping. MetaboLynx (Waters) was used to analyze the Q-TOF MS^E data.

■ ASSOCIATED CONTENT

Ⓢ Supporting Information

Structure of the 10 active molecules added to the library. This material is available free of charge via the Internet at http://pubs.acs.org.

■ AUTHOR INFORMATION

Corresponding Author

*Phone: 514-398-8543. Fax: 514-398-3797. E-mail: nicolas.moitessier@mcgill.ca.

Notes

The authors declare no competing financial interest.

■ ACKNOWLEDGMENTS

We thank AstraZeneca, NSERC, and CIHR for funding as well as the Faculty of Science (McGill University) for the Fessenden Professorship in Innovation to NM.

■ ABBREVIATIONS USED

AMC, aminocoumarin; BOP, benzotriazol-1-yl-oxy-tris-(dimethylamino)-phosphoniumhexafluorophosphate; DCM, dichloromethane; DMF, dimethylformamide; DMSO, dimethylsulfoxide; DPP, dipeptidyl peptidase; HLM, human liver microsomes; PBS, phosphate buffered saline; Piv, pivaloyl; POP, prolyl oligopeptidase; RLM, rat liver microsomes; TFA, trifluoroacetic acid; TFAA, trifluoroacetic anhydride; THF, tetrahydrofuran

■ REFERENCES

(1) Szeltner, Z.; Rea, D.; Juhasz, T.; Renner, V.; Fulop, V.; Polgar, L. Concerted Structural Changes in the Peptidase and the Propeller Domains of Prolyl Oligopeptidase are Required for Substrate Binding. *J. Mol. Biol.* **2004**, *340*, 627–637.

(2) Polgar, L. Unusual secondary specificity of prolyl oligopeptidase and the different reactivities of its two forms toward charged substrates. *Biochemistry* **1992**, *31*, 7729–7735.

(3) Bastos, I. M. D.; Grellier, P.; Martins, N. F.; Cadavid-Restrepo, G.; De Souza-Ault, M. R.; Augustyns, K.; Teixeira, A. R. L.; Schrével, J.; Maigret, B.; Da Silveira, J. F.; Santana, J. M. Molecular, functional and structural properties of the prolyl oligopeptidase of *Trypanosoma cruzi* (POP Tc80), which is required for parasite entry into mammalian cells. *Biochem. J.* **2005**, *388*, 29–38.

(4) Irazusta, J.; Larrinaga, G.; Gonz·lez-Maeso, J.; Gil, J.; Meana, J. J.; Casis, L. Distribution of prolyl endopeptidase activities in rat and human brain. *Neurochem. Int.* **2002**, *40*, 337–345.

(5) Szeltner, Z.; Polgar, L. Structure, function and biological relevance of prolyl oligopeptidase. *Curr. Protein Pept. Sci.* **2008**, *9*, 96–107.

(6) Männisto, P. T.; Vanäläinen, J.; Jalkanen, A.; Garcia-Horsman, J. A. Prolyl oligopeptidase: a potential target for the treatment of cognitive disorders. *Drug News Persp.* **2007**, *20*, 293–305.

(7) Brandt, I.; Scharpe, S.; Lambeir, A. M. Suggested functions for prolyl oligopeptidase: a puzzling paradox. *Clin. Chim. Acta* **2007**, *377*, 50–61.

(8) Williams, D. H.; O'Brien, D. P.; Sandercock, A. M.; Stephens, E. Order changes within receptor systems upon ligand binding: receptor tightening/oligomerisation and the interpretation of binding parameters. *J. Mol. Biol.* **2004**, *340*, 373.

(9) Lawandi, J.; Gerber-Lemaire, S.; Juillerat-Jeanneret, L.; Moitessier, N. Inhibitors of prolyl oligopeptidases for the therapy of human diseases: defining diseases and inhibitors. *J. Med. Chem.* **2010**, *53*, 3423–3438.

(10) Shinoda, M.; Toide, K.; Ohsawa, I.; Kohsaka, S. Specific inhibitor for prolyl endopeptidase suppresses the generation of amyloid ? protein in NG108–15 cells. *Biochem. Biophys. Res. Commun.* **1997**, *235*, 641–645.

(11) Laitinen, K. S. M.; Van Groen, T.; Tanila, H.; Venalainen, J.; Mannisto, P. T.; Alafuzoff, I. Brain prolyl oligopeptidase activity is associated with neuronal damage rather than beta-amyloid accumulation. *NeuroReport* **2001**, *12*, 3309–3312.

(12) Cunningham, D. F.; O'Connor, B. Identification and initial characterisation of a *N*-benzyloxycarbonyl-prolyl-prolinal (*Z*-Pro-prolinal)-insensitive 7-(*N*-benzyloxycarbonyl-glycyl-prolyl-amido)-4-methylcoumarin (*Z*-Gly-Bro-NH-Mec)-hydrolysing peptidase in bovine serum. *Eur. J. Biochem.* **1997**, *244*, 900–903.

(13) Kuhns, L. R.; Loder, R. T.; Farley, F. A.; Hensinger, R. N. Nuchal cord changes in children with os odontoideum: evidence for associated trauma. *J. Pediatr. Orthop.* **1998**, *18*, 815–819.

(14) Toide, K.; Shinoda, M.; Iwamoto, Y.; Fujiwara, T.; Okamiya, K.; Uemura, A. A novel propyl endopeptidase inhibitor, JTP-4819, with potential for treating Alzheimer's disease. *Behav. Brain Res.* **1997**, *83*, 147–151.

(15) Saito, M.; Hashimoto, M.; Kawaguchi, N.; Shibata, H.; Fukami, H.; Tanaka, T.; Higuchi, N. Synthesis and inhibitory activity of acyl-peptidyl-pyrrolidine derivatives toward post-proline cleaving enzyme; a study of subsite specificity. *J. Enzyme Inhib.* **1991**, *5*, 51.

(16) Barelli, H.; Petit, A.; Hirsch, E.; Wilk, S.; De Nanteuil, G.; Morain, P.; Checler, F. S-17092–1, a highly potent, specific and cell permeant inhibitor of human proline endopeptidase. *Biochem. Biophys. Res. Commun.* **1999**, *257*, 657–661.

(17) López, A.; Tarragó, T.; Giralt, E. Low molecular weight inhibitors of prolyl oligopeptidase: a review of compounds patented from 2003 to 2010. *Exp. Opin. Ther. Pat.* **2011**, *21*, 1023–1044.

(18) Miyazaki, A.; Toide, K.; Sasaki, Y.; Ichitani, Y.; Iwasaki, T. Effect of a prolyl endopeptidase inhibitor, JTP-4819, on radial maze performance in hippocampal-lesioned rats. *Pharmacol., Biochem. Behav.* **1998**, *59*, 361–368.

(19) Kato, A.; Fukunari, A.; Sakai, Y.; Nakajima, T. Prevention of amyloid-like deposition by a selective prolyl endopeptidase inhibitor, Y-29794, in senescence-accelerated mouse. *J. Pharmacol. Exp. Ther.* **1997**, *283*, 328−335.
(20) Umemura, K.; Kondo, K.; Ikeda, Y.; Kobayashi, T.; Urata, Y.; Nakashima, M. Pharmacokinetics and safety of JTP-4819, a novel specific orally active prolyl endopeptidase inhibitor, in healthy male volunteers. *Br. J. Clin. Pharmacol.* **1997**, *43*, 613−618.
(21) Jalkanen, A. J.; Hakkarainen, J. J.; Lehtonen, M.; Venäläinen, T.; Kääriäinen, T. M.; Jarho, E.; Suhonen, M.; Forsberg, M. M. Brain Pharmacokinetics of Two Prolyl Oligopeptidase Inhibitors, JTP-4819 and KYP-2047, in the Rat. *Basic Clin. Pharmacol. Toxicol.* **2011**, *109*, 443−451.
(22) Lawandi, J.; Toumieux, S.; Seyer, V.; Campbell, P.; Thielges, S.; Juillerat-Jeanneret, L.; Moitessier, N. Constrained peptidomimetics reveal detailed geometric requirements of covalent prolyl oligopeptidase inhibitors. *J. Med. Chem.* **2009**, *52*, 6672−6684.
(23) Kahyaoglu, A.; Haghjoo, K.; Kraicsovits, F.; Jordan, F.; Polgar, L. Benzyloxycarbonylprolylprolinal, a transition-state analogue for prolyl oligopeptidase, forms a tetrahedral adduct with catalytic serine, not a reactive cysteine. *Biochem. J.* **1997**, *322*, 839−843.
(24) Fülöp, V.; Böcskey, Z.; Polgar, L. Prolyl oligopeptidase: an unusual beta-propeller domain regulates proteolysis. *Cell* **1998**, *94*, 161.
(25) Moitessier, N.; Englebienne, P.; Lee, D.; Lawandi, J.; Corbeil, C. R. Towards the development of universal, fast and highly accurate docking/scoring methods: A long way to go. *Br. J. Pharmacol.* **2008**, 153.
(26) Singh, J.; Petter, R. C.; Baillie, T. A.; Whitty, A. The resurgence of covalent drugs. *Nature Rev. Drug. Discovery* **2011**, *10*, 307−317.
(27) *GOLD 3.0*; CCDC: Cambridge, UK, 2005.
(28) *AutoDock 4.0*; The Scripps Research Institute: La Jolla, CA, 2006.
(29) *FlexX 3.1.0*; BioSolveIT: Sankt Augustin, Germany, 2008.
(30) Corbeil, C. R.; Englebienne, P.; Moitessier, N. Docking ligands into flexible and solvated macromolecules. 1. Development and validation of Fitted 1.0. *J. Chem. Inf. Model.* **2007**, *47*, 435−449.
(31) Corbeil, C. R.; Englebienne, P.; Yannopoulos, C. G.; Chan, L.; Das, S. K.; Bilimoria, D.; L'Heureux, L.; Moitessier, N. Docking ligands into flexible and solvated macromolecules. 2. Development and application of Fitted 1.5 to the virtual screening of potential HCV polymerase inhibitors. *J. Chem. Inf. Model.* **2008**, *48*, 902−909.
(32) Fradera, X.; Kaur, J.; Mestres, J. Unsupervised guided docking of covalently bound ligands. *J. Comput.-Aided Mol. Des.* **2004**, *18*, 635−650.
(33) Katritch, V.; Byrd, C. M.; Tseitin, V.; Dai, D.; Raush, E.; Totrov, M.; Abagyan, R.; Jordan, R.; Hruby, D. E. Discovery of small molecule inhibitors of ubiquitin-like poxvirus proteinase I7L using homology modeling and covalent docking approaches. *J. Comput.-Aided Mol. Des.* **2007**, *21*, 549−558.
(34) Wang, J.; Wolf, R. M.; Caldwell, J. W.; Kollman, P. A.; Case, D. A. Development and testing of a general Amber force field. *J. Comput. Chem.* **2004**, *25*, 1157−1174.
(35) Englebienne, P.; Moitessier, N. Docking ligands into flexible and solvated macromolecules. 5. Force-field-based prediction of binding affinities of ligands to proteins. *J. Chem. Inf. Model.* **2009**, *49*, 2564−2571.
(36) Therrien, E.; Englebienne, P.; Arrowsmith, A. G.; Mendoza-Sanchez, R.; Corbeil, C. R.; Weill, N.; Campagna-Slater, V.; Moitessier, N. Integrating Medicinal Chemistry, Organic/Combinatorial Chemistry, and Computational Chemistry for the Discovery of Selective Estrogen Receptor Modulators with Forecaster, a Novel Platform for Drug Discovery. *J. Chem. Inf. Model.* **2012**, *52*, 210−224.
(37) Irwin, J. J.; Shoichet, B. K. ZINC—A Free Database of Commercially Available Compounds for Virtual Screening. *J. Chem. Inf. Model.* **2005**, *45*, 177−182.
(38) *A Free Database for Virtual Screening ZINC*; http://blaster.docking.org/zinc/ (Accessed Jan 03, 2012).
(39) Racys, D. T.; Rea, D.; Fülöp, V.; Wills, M. Inhibition of prolyl oligopeptidase with a synthetic unnatural dipeptide. *Bioorg. Med. Chem.* **2010**, *18*, 4775−4782.
(40) Juillerat-Jeanneret, L. Prolyl-specific peptidases and their inhibitors in biological processes. *Curr. Chem. Biol.* **2008**, *2*, 97−109.
(41) Kichik, N.; Tarrago, T.; Claasen, B.; Gairi, M.; Millet, O.; Giralt, E. 15N Relaxation NMR Studies of Prolyl Oligopeptidase, an 80 kDa Enzyme, Reveal a Pre-existing Equilibrium between Different Conformational States. *ChemBioChem* **2011**, *12*, 2737−2739.
(42) Kaszuba, K.; Róg, T.; Danne, R.; Canning, P.; Fülöp, V.; Juhász, T.; Szeltner, Z.; St. Pierre, J. F.; García-Horsman, A.; Männistö, P. T.; Karttunen, M.; Hokkanen, J.; Bunker, A. Molecular dynamics, crystallography and mutagenesis studies on the substrate gating mechanism of prolyl oligopeptidase. *Biochimie* **2012**, *94*, 1398−1411.
(43) Perron, Y. G.; Dewitt, N. Y.; Lee, C., Phthalamido penicillins, U.S. Patent 3,035,047 1962.
(44) McCormick, J. E.; McElhinney, R. S.; McMurry, T. B. H.; O'Brien, J. E. *N,N′*-Transphthaloylation in a Monoprotected Diamine. *Synthesis* **2006**, 983−988.